PHYSICAL REVIEW C **74**, 041301(R) (2006)

Shell corrections at the saddle point for mass ∼200

K. Mahata,* S. Kailas,† and S. S. Kapoor
Nuclear Physics Division, Bhabha Atomic Research Centre, Mumbai 400 085, India
(Received 31 October 2005; revised manuscript received 27 April 2006; published 26 October 2006)

Statistical model analysis of the measured evaporation residue and fission excitation functions indicates the presence of shell corrections to the liquid drop energy at the saddle point deformations for nuclei of mass ∼200, if one attempts to fit simultaneously the measured prefission neutron multiplicities.

DOI: 10.1103/PhysRevC.74.041301 PACS number(s): 25.70.Jj, 24.10.Pa, 24.75.+i, 27.80.+w

Determination of the height of the fission barrier (B_f), the saddle point deformation, and the shell corrections as a function of deformation continues to be a challenging problem [1]. It has ramifications for understanding the delicate interplay between the macroscopic aspect of the bulk nuclear matter and the quantal effects of a finite number of nucleons. The height of the fission barrier is a key ingredient in the description of heavy ion induced fusion fission reactions and in the prediction of the region of the relatively stable super heavy elements. Some specific applications, such as stellar nucleosynthesis, also require an accurate knowledge of the fission cross sections, which depend on the fission barrier heights (see Ref. [2] and references therein).

It is well established that the fission barriers of actinide nuclei have double-humped shapes due to the influence of the nuclear shell effects around the saddle point shapes. In nuclei of $A \sim 200$, shell corrections are not expected to lead to any significant secondary minimum in the nuclear deformation potential energy because of much steeper variation in the liquid drop energy with deformation. However, a significant shell correction may be present at the saddle point deformation of these nuclei, as indicated by some calculations [3–5]. Experimental information regarding the shell correction energy at the saddle point deformation for $A \sim 200$ is scarce.

Most measurements of fission cross sections for $A \sim 200$ are performed at energies much higher than that of the fission barrier height, where there are other competing open channels and a statistical description of the data is essential. In the statistical model, the choice between fission and evaporation of the light particle is governed by the relative density of levels (phase space) available for these two processes. For evaporation of the neutron, the level density is governed by the thermal energy (U_n) and the density of the single particle states at the Fermi energy in the ground state configuration of the residual nucleus. The available thermal energy is determined by the mass of the nuclei involved in the decay. For fission decay, the level density of the fissioning nucleus at the saddle point comes into play. The thermal energy (U_f) at the saddle point is determined by the fission barrier height (B_f). The single particle level density parameter at the saddle point (a_f) may be different from that for the ground state configuration (a_n), because of different nuclear shapes in the two cases. It has been shown [6] that there exists an excitation energy dependence of the nuclear shell effects on the level densities, which has been later parameterized by an excitation energy dependent level density parameter [7].

Although a number of studies have been made, there are still ambiguities in choosing various input parameters for the statistical model analysis. In earlier analyses of fission excitation functions to extract fission barrier heights, no attempt has been made to fit simultaneously the excitation functions of various evaporation residues and the number of prefission neutrons emitted in competition with fission. While the fission cross section, which is cumulative, can be fitted by several correlated pairs of B_f and a_f/a_n, the fission cross section and prefission neutron multiplicity can be fitted simultaneously by a unique pair only [8,9].

In this article, we present a statistical model analysis of the fission and the various evaporation residue cross sections along with the prefission neutron multiplicity for nuclei of $A \sim 200$ to extract fission barrier heights and infer shell correction at the saddle point in this region.

The data [9–13] considered in the present analysis (Table I) were chosen such that the contribution from noncompound events (e.g., preequilibrium, quasifission, fast fission) is not important and a statistical description is valid. We also restricted the excitation energy (E^*) range from 40 to 65 MeV, where fission dissipation effects leading to dynamical fission delays are expected to be less important. Statistical model calculations are performed using the code PACE [14] with a modified fission barrier and level density prescription. The fission barrier height can be written as

$$B_f = B_{\mathrm{LD}} - \Delta_n + \Delta_f, \tag{1}$$

where B_{LD}, Δ_n, and Δ_f are the liquid drop (LD) component of the fission barrier, the shell correction at the ground state, and the shell correction at the saddle point of the fissioning nuclei, respectively (see Fig. 1). The liquid drop component of the fission barrier is taken from the rotating finite range model (RFRM) [15]. The shell correction at the equilibrium deformation is obtained by

$$\Delta_n = M - M_{\mathrm{LD}} \tag{2}$$

where M and M_{LD} are the experimental and the liquid drop mass, respectively. The values of shell correction at the saddle deformation (Δ_f) are assumed to be $k_f \times \Delta_n$, where the

*Electronic address: kmahata@magnum.barc.ernet.in; present address: GSI, Planckstr. 1, D-64291 Darmstadt, Germany.
†Electronic address: kailas@magnum.barc.ernet.in.

TABLE I. The values of relevant statistical model parameters corresponding to the best fit without considering dynamical emission of neutrons (Set A) and with considering dynamical emission of neutrons with an assumed dynamical delay time of 30×10^{-21} s (Set B).

System	Set A $k_f, \tilde{a}_f/\tilde{a}_n$	Set B $k_f, \tilde{a}_f/\tilde{a}_n$	Δ_n (MeV)	Set A Δ_f (MeV)	Set B Δ_f (MeV)	Set A $B_f^{\exp}(0)$ (MeV)	Set B $B_f^{\exp}(0)$ (MeV)	$B_{\mathrm{LD}}(0)$ (MeV)
$^{16}\mathrm{O} + ^{181}\mathrm{Ta}$	1.09, 1.02	0.73, 1.04	−4.74	−5.17	−3.46	12.6	14.3	13.0
$^{16}\mathrm{O} + ^{182}\mathrm{W}$	1.00, 1.01	0.80, 1.02	−5.57	−5.57	−4.46	11.7	12.8	11.7
$^{12}\mathrm{C} + ^{198}\mathrm{Pt}$	0.86, 0.98	0.76, 1.00	−10.8	−9.29	−8.21	12.3	13.4	10.8
$^{12}\mathrm{C} + ^{194}\mathrm{Pt}$	0.83, 0.99	0.81, 1.00	−8.09	−6.71	−6.55	11.7	11.8	10.3
$^{19}\mathrm{F} + ^{192}\mathrm{Os}$	0.78, 1.01	0.68, 1.02	−8.64	−6.74	−5.88	11.6	12.4	9.67
$^{19}\mathrm{F} + ^{188}\mathrm{Os}$	0.74, 1.01	0.71, 1.02	−6.27	−4.64	−4.45	10.8	10.9	9.13
$^{19}\mathrm{F} + ^{198}\mathrm{Pt}$	0.82, 1.02	0.68, 1.03	−3.00	−2.46	−2.04	8.6	9.1	8.1
$^{19}\mathrm{F} + ^{194}\mathrm{Pt}$	0.64, 0.98	0.59, 1.00	−6.33	−4.05	−3.73	9.9	10.2	7.6

parameter k_f is to be determined by the fits to the experimental data. An energy dependent shell correction of the level density parameter [7]

$$a_x = \tilde{a}_x[1 + (\Delta_x/U_x)(1 - e^{-\eta U_x})] \tag{3}$$

is employed with $x = n$ or f corresponding to equilibrium or saddle deformation. The damping factor η is taken to be 0.054 MeV^{-1} [7]. The asymptotic liquid drop values $\tilde{a}_n$ and $\tilde{a}_f$ are taken to be $A/9$ MeV^{-1} and $\tilde{a}_f/\tilde{a}_n \times \tilde{a}_n$, respectively. The experimental masses are used to calculate the compound nucleus excitation energy and particle separation energy. The intrinsic excitation energy of the compound nucleus at the equilibrium configuration, U_n, is defined as $U_n = E^* - E_{\mathrm{rot}}(J) - \delta_p$, where E^*, $E_{\mathrm{rot}}(J)$, and δ_p are the total excitation energy, the rotational energy, and the pairing energy, respectively. The intrinsic excitation energy available at the saddle point deformation, U_f, is taken as $U_f = U_n - B_f$. The initial J distributions of the decaying compound nuclei are obtained from the fits to the experimental fusion excitation functions using the coupled channels code CCDEF [16].

The values of k_f and $\tilde{a}_f/\tilde{a}_n$ are varied to fit the experimental fission and xn evaporation residue excitation functions along with the prefission neutron multiplicities. The values of ν_{pre} are taken from the literature [17] and the systematics of Baba *et al.* [18], which is based on the experimental results. It is well recognized that contribution to ν_{pre} can also come from emission during dynamical delay in the fission process, in addition to that arising from statistical competition with fission. The dynamical neutrons can be emitted during the total dynamical delay comprised of compound nucleus formation time, transient delay time to reach the saddle, and saddle-to-scission time. As one extreme, one can assume that there are no dynamical neutrons and that these ν_{pre} values represent neutrons emitted statistically in competition with fission. Under this assumption, the values of k_f and $\tilde{a}_f/\tilde{a}_n$ that give the best fit to the evaporation residue, the fission, and the ν_{pre} data are given in Table I (Set A). As can be seen from Table I, under this assumption of zero dynamical neutrons, the present analysis resulted in a significant amount of shell correction at the saddle point. The uncertainties in the parameters obtained by the χ^2 minimization method are typically a few percent. It should be mentioned here that the values of $(k_f, \tilde{a}_f/\tilde{a}_n)$ are assumed to be the same for all the nuclei encountered during the decay process. These values are actually weighted averages over the decay steps, and from the variation in values of k_f for different compound nuclei with the same Z, an uncertainty of ∼5% can be assigned. These results are found to be less sensitive to the other parameters like $\tilde{a}_n$ and η. The values of k_f representing the shell corrections at the saddle point shown in Table I (Set A) are an upper limit, and these values can be smaller when one considers the presence of dynamical neutrons as discussed later.

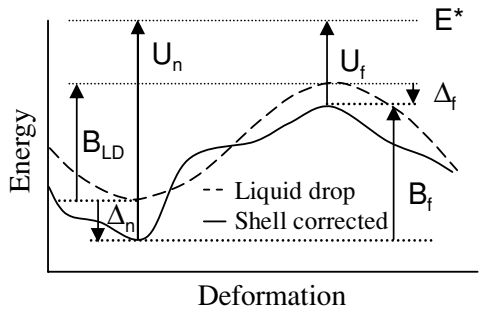

FIG. 1. A schematic representation of the potential energy of deformation of a nucleus with shell correction.

Fits to the fusion, the fission, and the xn evaporation residue excitation functions are shown in the top panels of each graph in Fig. 2 for the $^{12}\mathrm{C} + ^{194,198}\mathrm{Pt}$ and $^{19}\mathrm{F} + ^{188,192}\mathrm{Os}$ systems using the parameters given in Table I (Set A). It was found that equally good fits to the cross-section data could be obtained by varying $(k_f, \tilde{a}_f/\tilde{a}_n)$ pairs in a correlated way. For example, equally good fits to the cross-section data (not shown in the figure) could be also obtained by the $(k_f, \tilde{a}_f/\tilde{a}_n)$ pairs (1.00, 0.94), (0.50, 1.04), and (0.00, 1.09) for the $^{12}\mathrm{C} + ^{194}\mathrm{Pt}$ system. However, as can be seen from the bottom panel of the graph for the $^{12}\mathrm{C} + ^{194}\mathrm{Pt}$ system in Fig. 2, the statistical model predictions of ν_{pre} for these sets of parameters are quite different. The predicted ν_{pre} values decrease, going from the pair (1.00, 0.94) to the pair (0.00, 1.09). The same behavior is observed in other systems as can be seen from Figs. 2

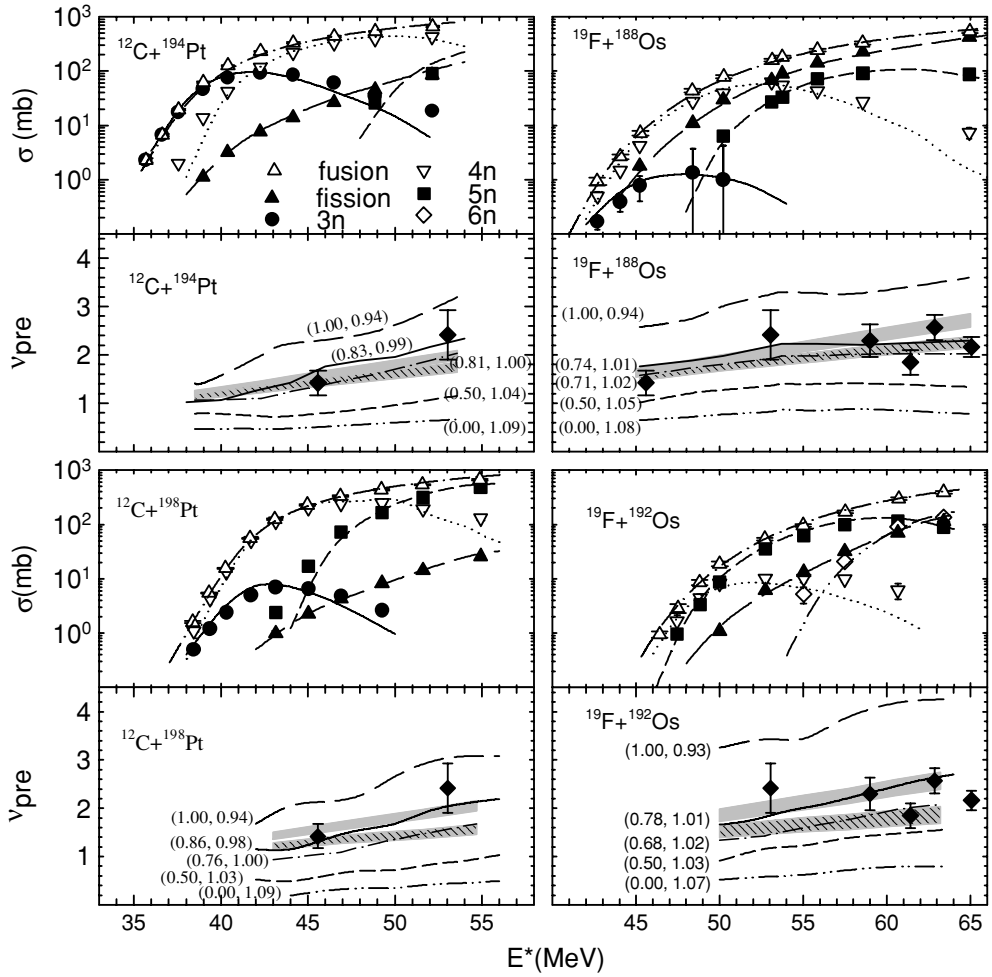

FIG. 2. (Top panels) The experimental fusion, evaporation residue, and fission excitation functions are compared with model calculations for the $^{12}C + ^{194,198}Pt$ and $^{19}F + ^{188,192}Os$ systems. The dot-dashed line represents the coupled channels calculation using CCDEF for fusion excitation function. The continuous, the dotted, the short dashed, the dot-dot-dashed, and the long dashed lines are the statistical model predictions for the $3n$, $4n$, $5n$, and $6n$ evaporations and the fission, respectively, using the parameters given in Table I (Set A). (Bottom panels) The statistical model predictions of prefission neutron multiplicities for various sets of values of $(k_f, \tilde{a}_f/\tilde{a}_n)$, which produce equally good fits to the ER and fission excitation functions, are compared with the data (filled diamonds) for $Z = 82$–87 [17] and the systematics [18] (gray band). The gray bands with diagonal lines are obtained from the systematics [18] (gray bands) after correction due to estimated dynamical neutron emission corresponding to a dynamical delay of 30×10^{-21} (see text).

and 3. Also shown in the bottom panel of each graph in Figs. 2 and 3 are the experimental values of ν_{pre} corresponding to $Z = 82$–87 [17] by solid diamond, the systematics of ν_{pre} (gray band) from the literature [18], and also the values of ν_{pre} after corrections for estimated emission of dynamical neutrons for an assumed dynamical delay time of 30×10^{-21} s (gray band with diagonal lines). A Monte Carlo procedure is used to estimate the above dynamical corrections. At each decay step, the mean lifetime of neutron emission (τ_n) is obtained from the neutron decay width (Γ_n). An actual time of decay is obtained by multiplying τ_n with the negative logarithm of a random number, chosen in the interval between 0 and 1 [19,20]. The correction due to dynamical emission is taken as the ratio of the number of neutrons emitted within the dynamical delay time to the total number of cascades. This dynamical delay time is the sum of the transient delay from the compound nucleus to the saddle point and the saddle-to-scission time. It can be seen that the contributions of the dynamical effects to the observed ν_{pre} values are rather small at the excitation energies spanned in Figs. 2 and 3. These corrections are reasonable upper limits estimated based on a dynamical delay of 30×10^{-21} s. Of course, the effects due to dynamical delay are significant at higher excitation energies [21]. The best fit parameters using the ν_{pre} corrected for an assumed dynamical delay time of 30×10^{-21} s are also given in Table I (Set B). It is clear that the ν_{pre} data are not consistent with the zero shell correction at the saddle point, unless one makes the extreme assumption that all the observed ν_{pre} arise because of dynamical delay. As this assumption requires unreasonably large dynamical delay times at these low excitation energy, it is reasonable to conclude that

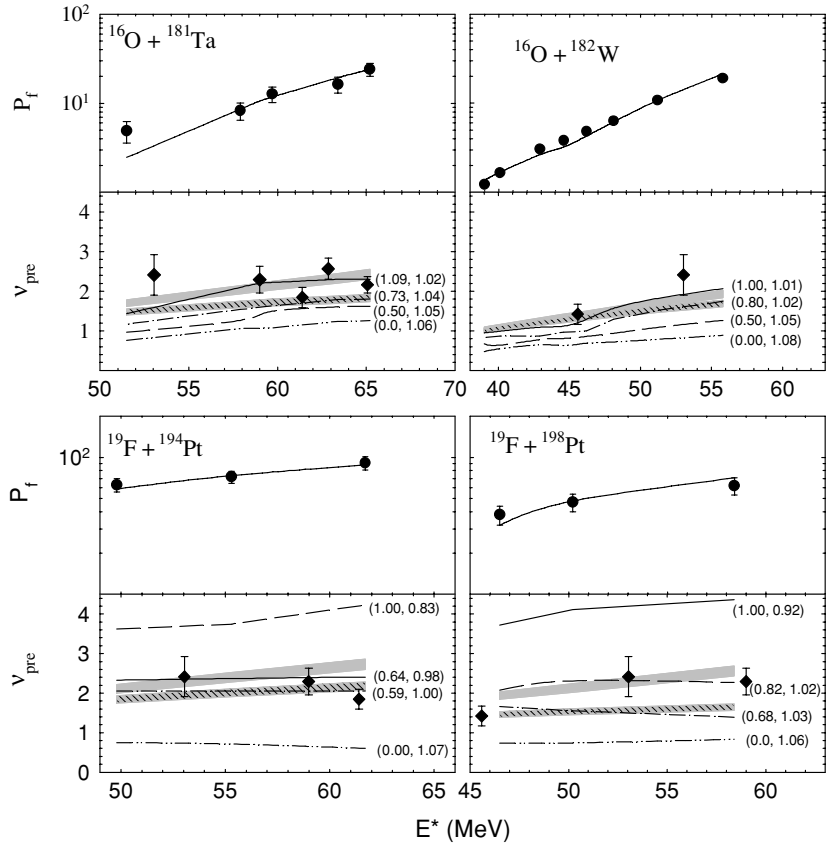

FIG. 3. (Top panels) The experimental fission probabilities are compared with the statistical model calculations for the $^{16}O + ^{181}Ta$, $^{16}O + ^{182}W$, and $^{19}F + ^{194,198}Pt$ systems. The continuous lines are the statistical model predictions for the fission probability using the parameters given in Table I (Set A). (Bottom panels) The statistical model predictions of prefission neutron multiplicities for various sets of values of $(k_f, \tilde{a}_f/\tilde{a}_n)$, which produce equally good fits to the fission probabilities, are compared with the data (filled diamonds) for $Z = 82$–87 [17] and the systematics [18] (gray bands). The gray bands with diagonal lines are obtained from the systematics [18] (gray bands) after correction due to estimated dynamical neutron emission corresponding to a dynamical delay of 30×10^{-21} (see text).

the ν_{pre} data point to a significant shell correction at the saddle point. Thus a minimum value of $k_f \sim 0.5-0.6$ is still required, even after making reasonable allowance for the presence of dynamical neutrons. A parameter set corresponding to $(k_f, \tilde{a}_f/\tilde{a}_n)$ of about 0.5–1.03 appears justifiable, taking into consideration dynamical neutrons, but this still corresponds to a significant shell correction at the saddle point equal to half of the ground state shell correction value. The corresponding ratio of the liquid drop part of the level density parameter $\tilde{a}_f/\tilde{a}_n$ is about 1.03, which is reasonable.

In the present analysis we do not explicitly take into account the possible collective enhancement of level densities that results in increased value of fission width and also the effect of Kramers factor [22] that, in contrast, decreases the value of fission width. A typical calculation with Kramers factor from 1 to 0.1 changes $(k_f, \tilde{a}_f/\tilde{a}_n)$ values from (0.78, 1.01) to (1.0, 1.09) for the $^{19}F + ^{192}Os$ system. Including collective enhancement according to Ref. [23] along with a Kramers factor of 0.1 changes the above values to (0.75, 0.93). It is noticed that the inclusion of Kramers and collective enhancement factors changes the $\tilde{a}_f/\tilde{a}_n$ values and the combined effect is to keep k_f nearly unchanged. The changes to fission width due to the above two factors go in opposite directions to essentially cancel the mutual effects. In a recent paper, Siwek-Wilczyńska *et al.* [24] have also shown from a statistical model analysis of fusion-fission data that there is no need for introduction of a pre-exponential factor (for Kramers and collective enhancement) to describe the data or that the presence of these factors is not brought out by the data in an energy range similar to that considered in the present analysis. It may be pointed out that the shell corrections at the saddle point were also deduced in Ref. [24] for compound nuclei with $Z = 88$–100 on the basis of Eq. (1), by using previously determined fission barriers and ground state shell corrections. These fission barriers were extracted in the past by fitting fission excitation functions alone on the basis of the statistical model, without considering the ν_{pre} values. Nevertheless, considering the overall behavior in the above range of Z values, it is stated that the shell effects practically vanish at the saddle configuration. But it can be seen from Fig. 6 of Ref. [24], that for the limited range of $Z = 88$–90, there are appreciable shell corrections at the saddle points. Thus the present results are not contradictory to the results shown in Fig. 6 of Ref. [24] with respect to the shell correction at the saddle point. The conclusion that, for fissionable nuclei in the range of $Z = 82$–90, a significant fraction of the ground state shell corrections persists at the saddle point is quite justified.

To summarize, a detailed statistical model analysis of the fission and the *xn* evaporation residue excitation functions along with the prefission neutron multiplicities was carried out. To the best of our knowledge, this is the first attempt to extract fission barrier and shell correction at the saddle point considering both cross-section and prefission neutron multiplicity data. The analysis has resulted in moderately strong shell corrections at the saddle point, at least about 50%

of that found at the ground state. Consequently, the fission barriers determined will differ from those obtained from earlier analyses without including the ν_{pre} data. Determination of fission cross section for individual chance (neutron fold in coincidence with fission) for these nuclei will elucidate these issues further. These results can provide a useful constraint for different models that are used to predict the fission barriers and the nuclear shapes at the extremes of charge, spin, and isospin.

One of us (S.S.K.) gratefully acknowledges the research support from the Indian National Science Academy (INSA).

[1] P. Möller, A. J. Sierk, and A. Iwamoto, Phys. Rev. Lett. **92**, 072501 (2004).
[2] *Handbook for calculations of nuclear reaction data: Reference input parameter library, RIPL-2*, IAEA-TECDOC-1506 (IAEA, Vienna, 2006).
[3] M. Bolsterli, O. E. Fiset, J. R. Nix, and J. L. Norton, Phys. Rev. C **5**, 1050 (1972).
[4] U. Mosel and H. W. Schmitt, Phys. Rev. C **4**, 2185 (1971).
[5] H. C. Pauli, T. Ledergerber, and M. Brack, Phys. Lett. **B34**, 264 (1971).
[6] V. S. Ramamurthy, S. S. Kapoor, and S. K. Kataria, Phys. Rev. Lett. **25**, 386 (1970).
[7] A. V. Ignatyuk, G. N. Smirenkin, and A. S. Tishin, Sov. J. Nucl. Phys. **21**, 255 (1975) [Yad. Fiz. **21**, 485 (1975)].
[8] S. E. Vigdor, H. J. Karwowski, W. W. Jacobs, S. Kailas, P. P. Singh, F. Soga, and P. Yip, Phys. Lett. **B90**, 384 (1980).
[9] K. Mahata, S. Kailas, A. Shrivastava, A. Chatterjee, A. Navin, P. Singh, S. Santra, and B. Tomar, Nucl. Phys. **A720**, 209 (2003).
[10] K. Mahata, S. Kailas, A. Shrivastava, A. Chatterjee, P. Singh, S. Santra, and B. S. Tomar, Phys. Rev. C **65**, 034613 (2002).
[11] A. Shrivastava, S. Kailas, A. Chatterjee, A. M. Samant, A. Navin, P. Singh, and B. S. Tomar, Phys. Rev. Lett. **82**, 699 (1999).
[12] B. R. Behera, S. Jena, M. Satpathy, S. Roy, P. Basu, M. K. Sharan, M. L. Chatterjee, S. Kailas, K. Mahata, and S. K. Datta, Phys. Rev. C **66**, 047602 (2002).
[13] D. J. Hinde, W. Pan, A. C. Berriman, R. D. Butt, M. Dasgupta, C. R. Morton, and J. O. Newton, Phys. Rev. C **62**, 024615 (2000).
[14] A. Gavron, Phys. Rev. C **21**, 230 (1980).
[15] A. J. Sierk, Phys. Rev. C **33**, 2039 (1986).
[16] J. Férnandez-Niello, C. H. Dasso, and S. Landowne, Comput. Phys. Commun. **54**, 409 (1989).
[17] D. J. Hinde, H. Ogata, M. Tanaka, T. Shimoda, N. Takahashi, A. Shinohara, S. Wakamatsu, K. Katori, and H. Okamura, Phys. Rev. C **39**, 2268 (1989).
[18] H. Baba, A. Shinohara, T. Saito, N. Takahashi, and A. Yokoyama, J. Phys. Soc. Jpn. **66**, 998 (1997).
[19] A. Gavron, A. Gayer, J. Boissevain, H. C. Britt, T. C. Awes, J. R. Beene, B. Cheynis, D. Drain, R. L. Ferguson, F. E. Obenshain *et al.*, Phys. Rev. C **35**, 579 (1987).
[20] H. Rossner, D. Hilscher, D. J. Hinde, B. Gebauer, M. Lehmann, M. Wilpert, and E. Mordhorst, Phys. Rev. C **40**, 2629 (1989).
[21] D. Hilscher and H. Rossner, Ann. Phys. Fr. **17**, 471 (1992).
[22] H. A. Kramers, Physica (Utrecht) **7**, 284 (1940).
[23] A. R. Junghans, M. de Jong, H. G. Clerc, A. V. Ignatyuk, G. A. Kudyaev, and K. H. Schmidt, Nucl. Phys. **A629**, 635 (1998).
[24] K. Siwek-Wilczyńska, I. Skwira, and J. Wilczyński, Phys. Rev. C **72**, 034605 (2005).